VNU Journal of Science: Mathematics – Physics, Vol. 38, No. 2 (2022) 91-105

VNU Journal of Science: Mathematics - Physics

Journal homepage: https://js.vnu.edu.vn/MaP

Original Article

# Dynamic Response of Sandwich Thick Plates with FG Face Sheets and Porous Core in Thermal Environments using Nonlocal Strain Gradient Theory Approach

Duong Tuan Manh, Do Thi Thu Ha*

*VNU University of Engineering and Technology, 144 Xuan Thuy, Cau Giay, Hanoi, Vietnam*

Received 11 November 2021
Revised 03 December 2021; Accepted 10 December 2021

**Abstract:** Based on nonlocal strain gradient theory approach, we have analyzed the nonlinear dynamic response and vibration of sandwich thick plates with functionally graded (FG) face sheets and FG porous core subjected to mechanical, thermal and blast loads on elastic foundations. Three types of porosity, including symmetric porosity distribution, non-symmetric porosity distribution, uniform porosity distribution have been considered of sandwich plate. The system of dynamic governing equations of motion is obtained by utilizing Hamilton's principle and solved by Bubnov-Galerkin method for a case of simply supported sandwich plate. Numerical results are presented and verified with other studies. The influence of nonlocal and strain gradient parameters, materials and porosity volume fraction, geometrical characteristics and parameters of elastic foundations on fundamental frequencies and dynamic response of the sandwich plates are elucidated.

*Keywords:* Sandwich Functionally Graded Materials (FGM) plates; Porous material; Dynamic response and Vibration; Nonlocal strain gradient theory.

## 1. Introduction

Sandwich structures are potential classes of composites consisting of a thick core layer and a thin cover layer for light weight and low flexural rigidity. Recently, academic works on the sandwich structures have been increasing rapidly in the light of its advanced mechanical properties and their wide application range in aviation, machinery, aerospace, medical, etc. Singh and Harsha [1] investigated the dynamic characteristics of a new sigmoid law based sandwich Functionally Graded Materials (FGM)

* Corresponding author.
*E-mail address:* dothithuha247@vnu.edu.vn

https//doi.org/10.25073/2588-1124/vnumap.4686

plate plates resting of Pasternak elastic foundation in the thermal environment based on stress-function Galerkin method. Adhikari et al. [2] proposed a higher order shear deformation theory to study the effect of porosity type defect and analyze the consequences of porosity on the buckling characteristic of various types of FGM sandwich combinations. Tomar and Talha [3] used Reddy's higher order shear deformation theory to investigate the influence of material uncertainties on vibration and bending behavior of skewed sandwich FGM plates. Research on the mechanics of structures containing porosities has been interested in recent years by other researchers. Rezaei et al. [4] dealt with the investigation of the free vibration analysis of rectangular plates composed of functionally graded materials with porosities by using a simple first order shear deformation plate theory. The nonlinear buckling and post-buckling characteristics of micro/nano-plates made of a porous FGM in the presence of non-locality and strain gradient size dependencies is analyzed in the work of Fan et al., [5].

Currently, various theoretical methods were conducted to study the linear and nonlinear stability, vibration, and dynamic responses of plates such as, the classical plate theory [6-7], the shear deformation theory [8-10], and the finite element theory [11-12]. Further, the non-classical continuum theories have been commonly used to investigate stability and dynamic response of micro/nanostructures. Hossein and Shirko [13] pointed out free vibration and wave propagation of thick plates based on the framework of the higher-order generalized nonlocal strain-gradient theory. Ebrahimi and Barati [14] presented a theoretical study on buckling analysis of graphene sheets under hydrothermal environments by a nonlocal strain gradient plate model.

Based on careful investigation in the available literature, most of the studies using the subject of the nonlocal gradient theory are focused on plates, beams and shell. It can be concluded that no study on sandwich thick plates with FG face sheets and porous core in thermal environments using nonlocal strain gradient theory approach has been conducted regardless of the high demand for understanding. This research considers effect of geometric parameter, material properties, foundation parameter, mechanical and thermal loads on the dynamic response of the sandwich plates.

## 2. Analytical Solution

### *2.1. Model Description and Material Properties*

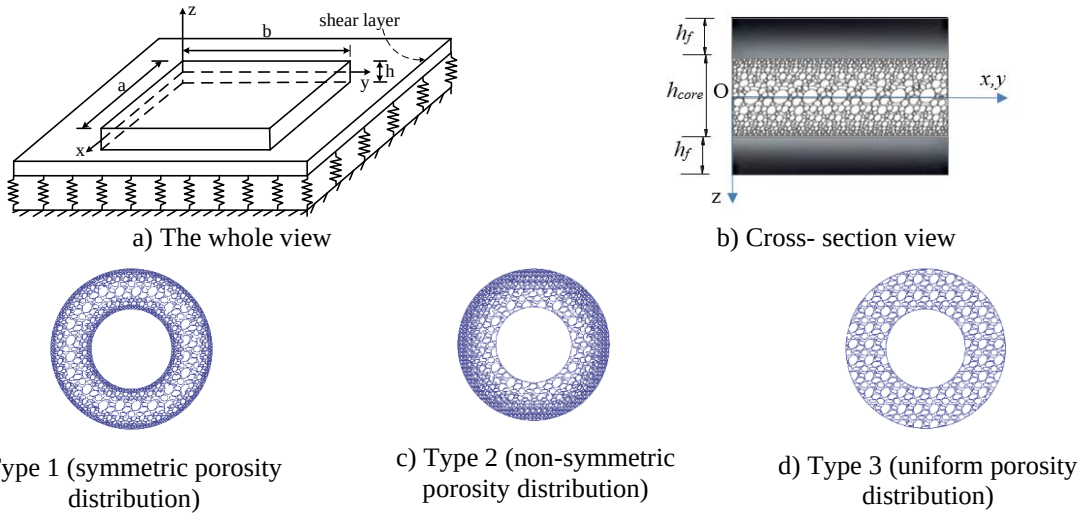


a) The whole view

b) Cross- section view

Type 1 (symmetric porosity distribution)

c) Type 2 (non-symmetric porosity distribution)

d) Type 3 (uniform porosity distribution)

Figure 1. The model of porous functionally graded sandwich plate on elastic foundations.

Consider a rectangular porous sandwich plate resting on elastic foundations as shown in Fig. 1a. The sandwich plate is composed of an FG-porous core and two similar FG face sheets that are assumed to be perfectly bonded to the core. The thickness of whole plate, top and bottom FGM face sheet and FG porous core are denoted by $h; h_f$ and $h_{core}$, respectively (Fig. 1b). The symbols $a$ and $b$ represent the length and width of the sandwich plate. A Cartesian coordinate system is established on the middle surface of the sandwich plate.

The variation of Young's modulus $E(z)$, thermal expansion coefficient $\alpha(z)$ and density $\beta(z)$ through the thickness direction of the sandwich plate are described by function as:

$$E(z)=\begin{cases} E_c+E_{mc}\left(\dfrac{2z+h}{h-h_{core}}\right)^k, & -\dfrac{h}{2}\le z\le -\dfrac{h_{core}}{2},\\ E_{core}, & -\dfrac{h_{core}}{2}\le z\le \dfrac{h_{core}}{2},\\ E_c+E_{mc}\left(\dfrac{2z-h}{h_{core}-h}\right)^k, & \dfrac{h_{core}}{2}\le z\le \dfrac{h}{2}, \end{cases}$$

$$\alpha(z)=\begin{cases} \alpha_c+\alpha_{mc}\left(\dfrac{2z+h}{h-h_{core}}\right)^k, & -\dfrac{h}{2}\le z\le -\dfrac{h_{core}}{2},\\ \alpha_{core}, & -\dfrac{h_{core}}{2}\le z\le \dfrac{h_{core}}{2},\\ \alpha_c+\alpha_{mc}\left(\dfrac{2z-h}{h_{core}-h}\right)^k, & \dfrac{h_{core}}{2}\le z\le \dfrac{h}{2}, \end{cases} \quad (1)$$

$$\rho(z)=\begin{cases} \rho_c+\rho_{mc}\left(\dfrac{2z+h}{h-h_{core}}\right)^k, & -\dfrac{h}{2}\le z\le -\dfrac{h_{core}}{2},\\ \rho_{core}, & -\dfrac{h_{core}}{2}\le z\le \dfrac{h_{core}}{2},\\ \rho_c+\rho_{mc}\left(\dfrac{2z-h}{h_{core}-h}\right)^k, & \dfrac{h_{core}}{2}\le z\le \dfrac{h}{2}, \end{cases}$$

where subscripts "*m*" and "*c*" represent for the metal and ceramic constituents, respectively. $k$ is volume fraction index ($0\le k<\infty$). $E_c$ and $E_m$ are elasticity modulus of ceramic and metal, and $\alpha_c$, $\alpha_m$ are thermal expansion coefficient of ceramic and metal, respectively.

+ Type1: symmetric porosity distribution

$$E_{core}=E_{\max}\left[1-e_0\cos\left(\frac{\pi z}{h_{core}}\right)\right],\ \alpha_{core}=\alpha_{\max}\left[1-e_0\cos\left(\frac{\pi z}{h_{core}}\right)\right],$$

$$\rho_{core}=\rho_{\max}\left[1-e_m\cos\left(\frac{\pi z}{h_{core}}\right)\right], \quad (2)$$

+ Type 2: non-symmetric porosity distribution

$$E_{core} = E_{\max}\left[1-e_0\cos\left(\frac{\pi z}{2h_{core}}+\frac{\pi}{4}\right)\right],\ \alpha_{core} = \alpha_{\max}\left[1-e_0\cos\left(\frac{\pi z}{2h_{core}}+\frac{\pi}{4}\right)\right],$$
$$\rho_{core} = \rho_{\max}\left[1-e_m\cos\left(\frac{\pi z}{2h_{core}}+\frac{\pi}{4}\right)\right], \quad (3)$$

+ + Type 3: uniform porosity distribution

$$E_{core} = E_{\max}\left(1-e_0\lambda_0\right),\ \alpha_{core} = \alpha_{\max}\left(1-e_0\lambda_0\right), \quad (4)$$

where z is the coordinate in the thickness direction; $0 \le e_0 \le 1$ is porosity parameter and can be obtained by $e_0 = 1-\frac{E_{\min}}{E_{\max}}$; $e_m = 1-\frac{\rho_{\min}}{\rho_{\max}}$; $0 \le e_m \le 1$. $E_{\min}; E_{\max}; \rho_{\min}; \rho_{\max}$ are respectively the minimum, maximum values of Young's modulus and mass density in the thickness direction of the plate, respectively.

The porous sandwich plate is assumed to rest on Pasternak – type elastic foundations. The interaction between the sandwich plate and elastic foundations is given as

$$q_f(x,y) = K_1 w - K_2\left(\frac{\partial^2 w}{\partial x^2}+\frac{\partial^2 w}{\partial y^2}\right), \quad (5)$$

in which $K_1$ and $K_2$ are respectively Winkler foundation modulus and the shear layer foundation stiffness of Pasternak model.

### *2.2. Theory and Formulations*

*The nonlocal strain gradient theory for sandwich plate*

The constitutive relationship corresponding to the total nonlocal strain gradient stress tensor considering thermal effects are given by [14-17]:

$$\sigma_{ij} = \sigma_{ij}^{(1)} - \nabla\sigma_{ij}^{(2)}, \quad (6)$$

where $\nabla$ is the gradient symbol; and $\sigma_{ij}^{(1)}$ and $\sigma_{ij}^{(2)}$ are the nonlocal stress and the higher-order nonlocal stress tensors, respectively.

The following expression of constitutive equation for nonlocal strain gradient theory [15]:

$$\left[1-(e_2a)^2\nabla^2\right]\left[1-(e_1a)^2\nabla^2\right]\sigma_{ij} = C_{ijkl}\left[1-(e_2a)^2\nabla^2\right]\varepsilon_{kl} - C_{ijkl}l^2\left[1-(e_1a)^2\nabla^2\right]\nabla^2\varepsilon_{kl} \quad (7)$$

where $\nabla^2$ is the Laplace operator.

When $e_1=e_2=e$, Eq. (7) is rewritten [14-17]:

$$\left[1-(ea)^2\nabla^2\right]\sigma_{ij} = \left(1-l^2\nabla^2\right)C_{ijkl}\varepsilon_{kl} \quad (8)$$

where $ea$ represents the nonlocal parameter.

*The classical plate theory*

In this research, the system of governing equations is established according the classical plate theory. The strain-displacement relations are defined as

$$\begin{bmatrix}\varepsilon_x\\ \varepsilon_y\\ \gamma_{xy}\end{bmatrix}=\begin{bmatrix}\varepsilon_x^0\\ \varepsilon_y^0\\ \gamma_{xy}^0\end{bmatrix}+z\begin{bmatrix}k_x\\ k_y\\ 2k_{xy}\end{bmatrix}=\begin{bmatrix}u_{,x}+\frac{1}{2}\left(w_{,x}\right)^2\\ v_{,y}+\frac{1}{2}\left(w_{,y}\right)^2\\ u_{,y}+v_{,x}+w_{,x}w_{,y}\end{bmatrix}+z\begin{bmatrix}-w_{,xx}\\ -w_{,yy}\\ -w_{,xy}\end{bmatrix} \tag{9}$$

The stress–strain relations including temperature effects, and the resultant moments and forces of the sandwich plate are expressed as:

$$\sigma_x=\frac{E(z)}{1-\nu^2}\left(\varepsilon_x+\nu\varepsilon_y\right)-\frac{E(z)\alpha(z)\Delta T}{1-\nu},$$
$$\sigma_y=\frac{E(z)}{1-\nu^2}\left(\varepsilon_y+\nu\varepsilon_x\right)-\frac{E(z)\alpha(z)\Delta T}{1-\nu}$$
$$\sigma_{xy}=\frac{E(z)}{2\left(1+\nu\right)}\gamma_{xy} \tag{10}$$
$$\left(M_x,M_y,M_{xy}\right)=\int_{-\frac{h}{2}}^{\frac{h}{2}}\left(\sigma_x,\sigma_y,\sigma_{xy}\right)zdz$$

The governing system of motion of the sandwich plate via Hamilton's principle can be defined as the following form [16, 17]:

$$N_{x,x}+N_{xy,y}=I_0\frac{\partial^2 u}{\partial t^2}, \tag{11}$$

$$N_{xy,x}+N_{y,y}=I_0\frac{\partial^2 v}{\partial t^2}, \tag{12}$$

$$M_{x,xx}+2M_{xy,xy}+M_{y,yy}+N_x^0w_{,xx}+2N_{xy}^0w_{,xy}+N_y^0w_{,yy}-q_f+q=I_0\frac{\partial^2 w}{\partial t^2} \tag{13}$$

where the mass inertia term is determined as $I_0=\int_{-\frac{h}{2}}^{\frac{h}{2}}\rho(z)dz$ and $q=Q\sin(\Omega t)$ ($Q$ is the amplitude of uniformly excited load, $\Omega$ is the frequency of the load).

The equations of motion of sandwich plate resting on elastic foundation can be derived in terms of displacement components *u*, *v* and *w* according to nonlocal strain gradient theory as follow

$$A_{11}\left[\frac{\partial^2 u}{\partial x^2}-l^2\left(\frac{\partial^4 u}{\partial x^4}+\frac{\partial^4 u}{\partial y^2\partial x^2}\right)\right]+A_{12}\left[\frac{\partial^2 v}{\partial y\partial x}-l^2\left(\frac{\partial^4 v}{\partial y\partial x^3}+\frac{\partial^4 v}{\partial y^3\partial x}-\frac{1}{R}\frac{\partial^3 w}{\partial y^2\partial x}-\frac{1}{R}\frac{\partial^3 w}{\partial x^3}\right)-\frac{1}{R}\frac{\partial w}{\partial x}\right]$$
$$+A_{33}\left[\frac{\partial^2 u}{\partial y^2}-l^2\left(\frac{\partial^4 u}{\partial y^2\partial x^2}+^2\frac{\partial^4 u}{\partial y^4}\right)-l^2\left(\frac{\partial^4 v}{\partial y\partial x^3}+\frac{\partial^4 v}{\partial y^3\partial x}\right)+\frac{\partial^2 v}{\partial y\partial x}\right]$$
$$+B_{11}\left[l^2\left(\frac{\partial^5 w}{\partial y^2\partial x^3}+\frac{\partial^5 w}{\partial x^5}\right)-\frac{\partial^3 w}{\partial x^3}\right]+B_{12}\left[l^2\left(\frac{\partial^5 w}{\partial y^4\partial x}+\frac{\partial^5 w}{\partial y^2\partial x^3}\right)-\frac{\partial^3 w}{\partial y^2\partial x}\right]$$
$$+B_{33}\left[l^2\left(\frac{\partial^5 w}{\partial y^4\partial x}+\frac{\partial^5 w}{\partial y^2\partial x^3}\right)-\frac{\partial^3 w}{\partial y^2\partial x}\right]=\left[1-(ea)^2\nabla^2\right]I_0\frac{\partial^2 u}{\partial t^2}, \tag{14}$$

$$A_{21}\left[\frac{\partial^2 u}{\partial y\partial x}-l^2\left(\frac{\partial^4 u}{\partial y\partial x^3}+\frac{\partial^4 u}{\partial y^3\partial x}\right)\right]+A_{22}\left\{\frac{1}{R}\left[l^2\left(\frac{\partial^3 w}{\partial y\partial x^2}+\frac{\partial^3 w}{\partial y^3}\right)-\frac{\partial w}{\partial y}\right]+\frac{\partial^2 v}{\partial y^2}-l^2\left(\frac{\partial^4 v}{\partial y^4}+\frac{\partial^4 v^1}{\partial y^2\partial x^2}\right)\right\}$$
$$+A_{33}\left[\frac{\partial^2 u}{\partial y\partial x}-l^2\left(\frac{\partial^4 u}{\partial y^3\partial x}+\frac{\partial^4 u}{\partial y\partial x^3}\right)+\frac{\partial^2 v}{\partial x^2}-l^2\left(\frac{\partial^4 v}{\partial x^4}+\frac{\partial^4 v}{\partial y^2\partial x^2}\right)\right]$$
$$+B_{21}\left[l^2\left(\frac{\partial^5 w}{\partial y^3\partial x^2}+\frac{\partial^5 w}{\partial y\partial x^4}\right)-\frac{\partial^3 w}{\partial y\partial x^2}\right]+B_{22}\left[l^2\left(\frac{\partial^5 w}{\partial y^3\partial x^2}+\frac{\partial^5 w}{\partial y^5}\right)-\frac{\partial^3 w}{\partial y^3}\right]$$
$$+B_{33}\left[l^2\left(\frac{\partial^5 w}{\partial y^3\partial x^2}+\frac{\partial^5 w}{\partial y\partial x^4}\right)-\frac{\partial^3 w}{\partial y\partial x^2}\right]=\left[1-(ea)^2\nabla^2\right]I_0\frac{\partial^2 v}{\partial t^2}, \tag{15}$$

$$\frac{A_{21}}{R}\left[\frac{\partial u}{\partial x}-l^2\left(\frac{\partial^3 u}{\partial x^3}+\frac{\partial^3 u}{\partial y^2\partial x}\right)\right]+\frac{A_{22}}{R}\left\{\frac{1}{R}\left[l^2\left(\frac{\partial^2 w}{\partial x^2}+\frac{\partial^2 w}{\partial y^2}\right)-w\right]+\frac{\partial v}{\partial y}-l^2\left(\frac{\partial^3 v}{\partial y^3}+\frac{\partial^3 v}{\partial y\partial x^2}\right)\right\}$$
$$+B_{11}\left[\frac{\partial^3 u}{\partial x^3}-l^2\left(\frac{\partial^5 u}{\partial x^5}+\frac{\partial^5 u}{\partial y^2\partial x^3}\right)\right]+B_{12}\left\{\left[\frac{\partial^3 v}{\partial y\partial x^2}-l^2\left(\frac{\partial^5 v}{\partial y^3\partial x^2}+\frac{\partial^5 v}{\partial y\partial x^4}\right)\right]\right.$$
$$\left.+\frac{1}{R}\left[l^2\left(\frac{\partial^4 w}{\partial y^2\partial x^2}+\frac{\partial^4 w}{\partial x^4}\right)-\frac{\partial^2 w}{\partial x^2}\right]\right\}+B_{21}\left\{\frac{\partial^3 u}{\partial y^2\partial x}-l^2\left(\frac{\partial^5 u}{\partial y^2\partial x^3}+\frac{\partial^5 u}{\partial y^4\partial x}\right)\right.$$
$$\left.+\frac{1}{R}\left[l^2\left(\frac{\partial^4 w}{\partial y^2\partial x^2}+\frac{\partial^4 w}{\partial x^4}\right)-\frac{\partial^2 w}{\partial x^2}\right]\right\}+D_{11}\left[l^2\left(\frac{\partial^6 w}{\partial x^6}+\frac{\partial^6 w}{\partial y^2\partial x^4}\right)-\frac{\partial^4 w}{\partial x^4}\right]$$
$$+D_{12}\left[l^2\left(\frac{\partial^6 w}{\partial y^4\partial x^2}+\frac{\partial^6 w}{\partial y^2\partial x^4}\right)-\frac{\partial^4 w}{\partial y^2\partial x^2}\right]+D_{21}\left[l^2\left(\frac{\partial^6 w}{\partial y^4\partial x^2}+\frac{\partial^6 w}{\partial y^2\partial x^4}\right)-\frac{\partial^4 w}{\partial y^2\partial x^2}\right]$$
$$+B_{22}\left\{\frac{2}{R}\left[l^2\left(\frac{\partial^4 w}{\partial y^2\partial x^2}+\frac{\partial^4 w}{\partial y^4}\right)-\frac{\partial^2 w}{\partial y^2}\right]-l^2\left(\frac{\partial^5 v}{\partial y^3\partial x^2}+\frac{\partial^5 v}{\partial y^5}\right)+\frac{\partial^3 v}{\partial y^3}\right\}$$
$$+2B_{66}\left[\frac{\partial^3 u}{\partial y^2\partial x}+\frac{\partial^3 v}{\partial y\partial x^2}-l^2\left(\frac{\partial^5 u}{\partial y^2\partial x^3}+\frac{\partial^5 v}{\partial y\partial x^4}+\frac{\partial^5 v}{\partial y^3\partial x^2}+\frac{\partial^5 u}{\partial y^4\partial x}\right)\right]$$
$$+D_{22}\left[l^2\left(\frac{\partial^6 w}{\partial y^6}+\frac{\partial^6 w}{\partial y^4\partial x^2}\right)-\frac{\partial^4 w}{\partial y^4}\right]+2D_{66}\left[l^2\left(\frac{\partial^6 w}{\partial y^2\partial x^4}+\frac{\partial^6 w}{\partial y^4\partial x^2}\right)-\frac{\partial^4 w}{\partial y^2\partial x^2}\right]$$

$$+\left[1-(ea)^2\left(\frac{\partial^2 w}{\partial x^2}+\frac{\partial^2 w}{\partial y^2}\right)\right]\left(N_x^0\frac{\partial^2 w}{\partial x^2}+2N_{xy}^0\frac{\partial^2 w}{\partial x\partial y}+N_y^0\frac{\partial^2 w}{\partial y^2}\right)$$
$$-\left[1-(ea)^2\left(\frac{\partial^2 w}{\partial x^2}+\frac{\partial^2 w}{\partial y^2}\right)\right]\left[K_1 w-K_2\left(\frac{\partial^2 w}{\partial x^2}+\frac{\partial^2 w}{\partial y^2}\right)\right]$$
$$+\left[1-(ea)^2\left(\frac{\partial^2 w}{\partial x^2}+\frac{\partial^2 w}{\partial y^2}\right)\right]q=\left[1-(ea)^2\left(\frac{\partial^2 w}{\partial x^2}+\frac{\partial^2 w}{\partial y^2}\right)\right]I_0\frac{\partial^2 w}{\partial t^2}. \quad (16)$$

*2.3. Closed- form Solutions*

*Boundary conditions and solution procedure*

Four edges of the porous sandwich plate are simply supported or clamped. The displacement and force boundary conditions are described as [17]:

- For simply supported

$$w=0,\ M_x=0,\ N_x=N_x^0 \text{ at } x=0,\ x=a \quad (17)$$
$$w=0,\ M_y=0,\ N_y=N_y^0 \text{ at } y=0,\ y=b$$

- For clamped

$$u=0,\ v=0,\ w=0,\ \frac{\partial w}{\partial x}=0 \text{ at } x=0,\ x=a \quad (18)$$
$$u=0,\ v=0,\ w=0,\ \frac{\partial w}{\partial y}=0 \text{ at } y=0,\ y=b$$

In this research, the analytical solutions satisfying the boundary conditions are assumed in the following forms:

$$u=U(t)\cos\frac{m\pi x}{a}\sin\frac{n\pi y}{b},\ v=V(t)\sin\frac{m\pi x}{a}\cos\frac{n\pi y}{b},\ w=W(t)\sin\frac{m\pi x}{a}\sin\frac{n\pi y}{b}, \quad (19)$$

where *m* and *n* are the number of half-waves in the orthogonal directions $x, y$ and *U(t), V(t)* , and *W(t)* are the time - dependent amplitudes.

By substituting Eq. (30) into Eqs. (14-16), then applying Galerkin's method, we have:

$$h_{11}U+h_{12}V+h_{13}W=\eta_1\frac{\partial^2 U}{\partial t^2}, \quad (20)$$

$$h_{21}U+h_{22}V+h_{23}W=\eta_1\frac{\partial^2 V}{\partial t^2}, \quad (21)$$

$$h_{31}U+h_{32}V+(h_{33}+h_{34}N_x^0+h_{35}K_1+h_{36}K_2)W+h_{37}q=\eta_1\frac{\partial^2 W}{\partial t^2} \quad (22)$$

where the details of coefficients $h_{ij}$ $(i=\overline{1,3};\ j=\overline{1,7})$ and $\eta_k$ $(k=\overline{1,3})$ may be found in Appendix 3.

*Natural frequency*

Considering linear terms of the system Eqs. (31) and setting q=0, three values of natural frequencies of the porous sandwich plate can be determined by solving following equation:

$$\begin{vmatrix} h_{11} & h_{12} & h_{13} \\ h_{21} & h_{22} & h_{23} \\ h_{31} & h_{32} & h_{33}+h_{34}N_x^0+h_{35}K_1+h_{36}K_2 \end{vmatrix}=0 \tag{23}$$

The smallest value of three solutions from Eq. (23) is considered.

## 3. Results and Discussion

To evaluate the reliability of the calculation, we compare the dimensionless natural frequency parameter $\varpi=\dfrac{\omega b^2}{h}\sqrt{\dfrac{\rho_0}{E_0}}$ with the numerical results of Li et al. [18] based on different theories including classical plate theory (CPT), the first order shear deformation plate theory (FSDT), sinusoidal shear deformation plate theory (SSDT), third order shear deformation plate theory (TSDT) and three dimensional linear theory (TDLT) (Table 1).

Table 1. Comparison study of dimensionless natural frequency parameter $\varpi=\dfrac{\omega b^2}{h}\sqrt{\dfrac{\rho_0}{E_0}}$

| k | Theories | The ratio thickness of each layer | | |
|---|---|---|---|---|
| | | 1-0-1 | 1-1-1 | 1-2-1 |
| 0.5 | Present | 1.46380 | 1.53349 | 1.58089 |
| | CPT [18] | 1.47157 | 1.54903 | 1.60722 |
| | FSDT [18] | 1.47157 | 1.51695 | 1.57274 |
| | TSDT [18] | 1.44424 | 1.51922 | 1.57451 |
| | TDLT [18] | 1.44614 | 1.52131 | 1.57668 |
| | SSDT [18] | 1.44436 | 1.59127 | 1.57450 |

Geometrical parameters of sandwich plates with FGM face sheet for the investigation as follows: $E_c=380\,GPa,\ \rho_c=3800\,kg/m^3, \alpha_c=7.4\times10^{-6}\left(^\circ K^{-1}\right), E_m=70\,GPa,\ \rho_m=2707\,kg/m^3,$ $\alpha_m=23\times10^{-6}\left(^\circ K^{-1}\right), a/b=1,\ h/b=0.1, \rho_0=1\ kg/m^3,\ E_0=1\ GPa,\ \ e_0=0,$ Poisson's ratio $\nu=0.3.$

As can be seen, our results are reliable with other published results ensuring the accuracy of the present method.

The results below evaluate the influence of elastic foundation, geometrical parameters, material parameters, and temperature on the dynamic response and natural frequency of sandwich plates under uniformly distributed transverse load and blast load.

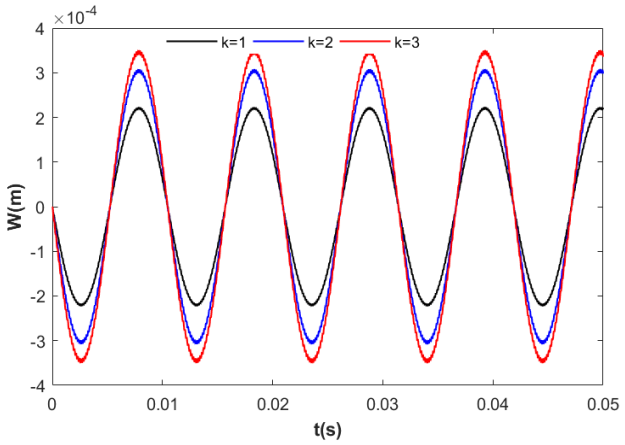


Figure 2. Influence of power law index *k* on the dynamic response.

Figure 2 indicates the effects of the power law index *k* on the nonlinear dynamic response of porous sandwich plate. The deflection amplitude of functionally graded sandwich plate increases when increasing the power law index. It is explained that if the value of volume fraction increases, the volume of ceramic component of sandwich increases. In addition, the elastic modulus of ceramic is higher than metal of this ones, which means that power law index increases leading to increase elastic modulus of structure. This reason results in the decreasing of the deflection amplitude of porous FGM plate.

Figure 3 shows the effects of the porosity coefficient $e_0$ on the nonlinear dynamic response of the FG sandwich plate. It is easy to see that the sandwich plate with the lower porosity coefficient has better stiffness. In addition, the higher porosity coefficient is, the higher deflection amplitude of the FG sandwich plate is. The deflection amplitude of the FG sandwich plate without porosity is smallest.

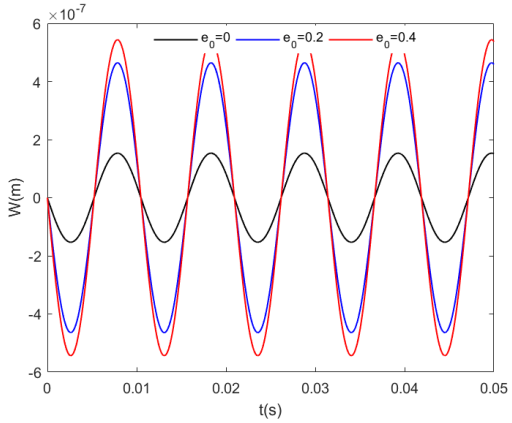


Figure 3. Effect of coefficient of plate porosity $e_0$ ratio on the time responses.

Figures 4 and 5 demonstrate the impact of the geometric parameters such as the plate length to width ratio $a/b$ and length to thickness ratio $a/h$ on the behavior of sandwich plates with porous core and FG face layer in thermal environment. It can be seen that the $a/b$ ratio decreases or $a/b$ ratio increases, the deflection amplitude of the porous functionally graded sandwich plate increases significantly. From

these results, it could be deduced that the stiffness of the functionally graded sandwich plate becomes weaker when $a/h$ ratio increases or $a/b$ ratio decreases.

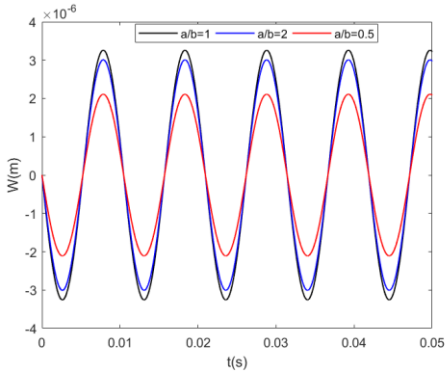


Figure 4. Influence of ratio *a/b* on the dynamic response.

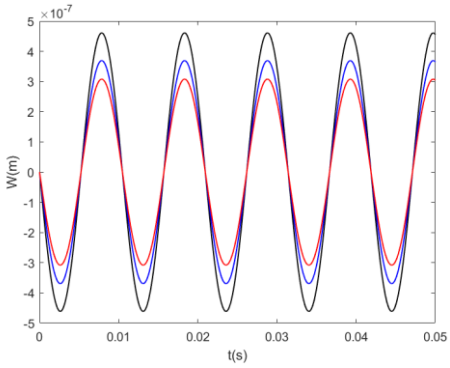


Figure 5. Influence of ratio *a/h* on the dynamic response.

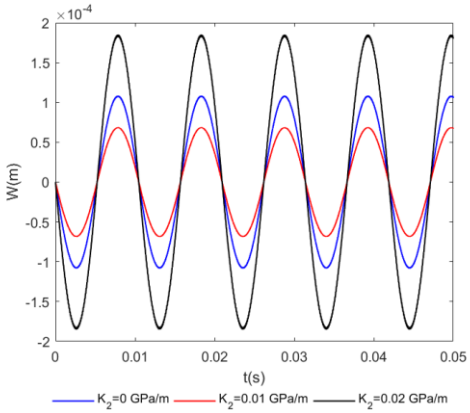


Figure 6. Influence of Pasternak foundation on the dynamic response.

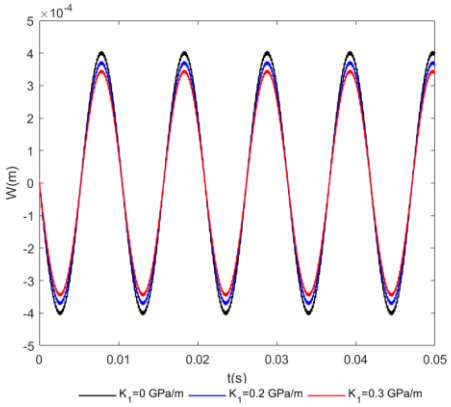


Figure 7. Influence of Winkler foundation on the dynamic response.

Figures 6 and 7 demonstrate the effect of the Winkler and Pasternak foundations on the dynamic response of the plate. From two figures, we can see that the modulus of the elastic foundation has beneficial effect on the deflection amplitude. On the other hand, it is easy to see that the plate becomes stiffer with support of elastic foundation.

We consider the effects of porosity ratio on dynamic response of sandwich plate with porous core and FG face sheets under blast loading [19] as following function:

$$q(t) = 1.8Ps_{max}\left(1-\frac{t}{T_s}\right)exp\left(\frac{-bt}{T_s}\right),$$

where the "1.8" factor accounts for the effects of a hemispherical blast, $Ps_{max}$ is the maximum static over-pressure, $b$ is the parameter controlling the rate of wave amplitude decay and $T_s$ is the parameter characterizing the duration of the blast pulse.

The influence of porosity ratio on dynamic response of sandwich plates with porous core and FG face sheets subjected blast loading $q = 1.8.290.100.\left(1-\frac{t}{0.005}\right).\exp\left(\frac{-2t}{0.005}\right)$ investigated and showed in Figure 8. It can be seen that increase of porosity coefficient leads to increase of the dynamic deflection.

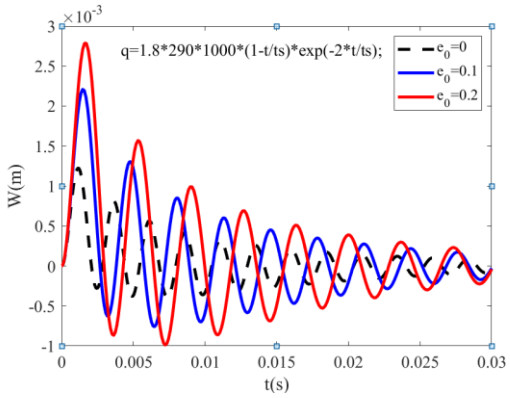


Figure 8. Influence of porosity on the dynamic response of sandwich plate subjected to blast loading.

Plots in Figure 9 reflect the influence of temperature on dynamic response of sandwich plates. This figure shows that with increasing the temperature changes, the dynamic deflection of the sandwich plate increases.

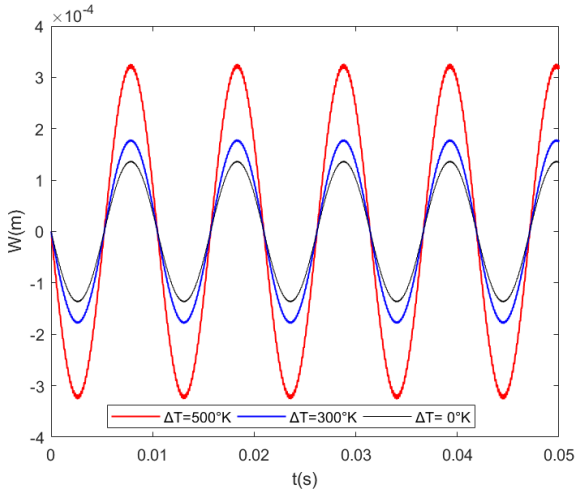


Figure 9. Effect of temperature increment $\Delta T$ on the time responses.

## 4. Conclusion

This work investigated the nonlinear dynamic response sandwich thick plates with porous core and FG face layers under mechanical and blast loading on elastic foundations based on a non local theory. Numerical results for the dynamic response of the plates are obtained by using Runge-Kutta method. The conclusions are obtained from this study:

• The natural frequency results of this work have been compared with other studies.

• The existence of porosity reduces the stiffness of FG sandwich plate. Consequently, the deflection amplitude increases and the natural frequency decreases as the porosity coefficient rises

• The foundation and stiffeners have positive impact on time-amplitude response curves of the plates.

• The temperature has significant impact on the nonlinear dynamic response of sandwich plates with porous core and FG face sheets. In addition, the temperature increment has negative effect on the amplitudes of the plates.

• The geometrical parameter, volume ratio index, mechanical and blast loads have been conducted.

## Acknowledgments

This research is funded by the Grant number CN.21.02 of the University of Engineering and Technology, VNU Hanoi. The authors are grateful for this support.

## References

[1] S. J. Singh, S. P. Harsha, Nonlinear Dynamic Analysis of Sandwich S-FGM Plate Resting on Pasternak Foundation under Thermal Environment, Eur J Mech A/Solids, Vol. 76, 2019, pp. 155-179, https://doi.org/10.1016/j.euromechsol.2019.04.005.

[2] B. Adhikari, P. Dash, B. N. Singh, Buckling Analysis of Porous FGM Sandwich Plates under Various Types Non-uniform Edge Compression Based on Higher Order Shear Deformation Theory. Compos Struct, Vol. 251, 2020, pp. 112597, https://doi.org/10.1016/j.compstruct.2020.112597.

[3] S. S. Tomar, M. Talha. Influence of Material Uncertainties on Vibration and Bending Behaviour of Skewed Sandwich FGM Plates. Compos Part B Eng, Vol. 163, 2019, pp.779-793, https://doi.org/10.1016/j.compositesb.2019.01.035.

[4] A. S. Rezaei, A. R. Saidi, M. Abrishamdari, M. P. H. Mohammadi, Natural Frequencies of Functionally Graded Plates with Porosities via A Simple Four Variable Plate Theory : An Analytical Approach. Thin Walled Struct, Vol. 120, 2017, pp. 366-377,https://doi.org/10.1016/j.tws.2017.08.003.

[5] F. Fan , B. Safaei , S. Sahmani, Buckling and Postbuckling Response of Nonlocal Strain Gradient Porous Functionally Graded Micro/nano-plates via NURBS-Based Isogeometric Analysis. Thin-Walled Struct, Vol. 159, 2021, pp. 107231, https://doi.org/10.1016/j.tws.2020.107231.

[6] N. D. Duc, Nonlinear Static and Dynamic Stability of Functionally Graded Plates and Shells, Vietnam Vietnam Natl Univ Press. 2014, pp. 724.

[7] N. D. Duc, V. D. Quang, P. D. Nguyen, T. M. Chien, Nonlinear Dynamic Response of Functional Graded Porous Plates on Elastic Foundation Subjected to Thermal and Mechanical Loads, J. Appl. Comput. Mech, Vol. 4, 2018, pp. 245-259, https://doi.org/10.22055/jacm.2018.23219.1151.

[8] S. Amir, M. Khorasani, H. B. A. Zarei, Buckling Analysis of Nanocomposite Sandwich Plates with Piezoelectric Face Sheets Based on Flexoelectricity and First-Order Shear Deformation Theory, J. Sandw. Struct. Mater.Vol. 22, 2018, pp. 2186-2209, https://doi.org/10.1177/1099636218795385.

[9] H. T. Thai, T. K. Nguyen, T. P. Vo, J. Lee, Analysis of Functionally Graded Sandwich Plates using A New First-Order Shear Deformation Theory, Eur. J. Mech. - A/Solids. , Vol. 45, 2014, pp. 211-225, https://doi.org/10.1016/j.euromechsol.2013.12.008.

[10] N. D. Duc, V. D. Quang, P. D. Nguyen, T. M. Chien, Nonlinear Dynamic Response of Functional Graded Porous Plates on Elastic Foundation Subjected to Thermal and Mechanical Loads, J. Appl. Comput. Mech, Vol. 4, 2018, pp. 245-259, https://doi.org/10.22055/jacm.2018.23219.1151.

[11] M. A. Shahmohammadi, M. Azhari, M. M. Saadatpour, S. S. Foroushani, Geometrically Nonlinear Analysis of Sandwich FGM and Laminated Composite Degenerated Shells Using The Isogeometric Finite Strip Method. Comput Methods Appl Mech Eng, Vol. 371, 2020, pp. 113311, https://doi.org/10.1016/j.cma.2020.113311.

[12] M. Ganapathi, S. Aditya, S. Shubhendu, O. Polit, Z. T. Ben, Nonlinear Supersonic Flutter Study of Porous 2D Curved Panels Including Graphene Platelets Reinforcement Effect Using Trigonometric Shear Deformable Finite Element. Int J Non Linear Mech Vol. 125, 2020, pp. 103543, https://doi.org/10.1016/j.ijnonlinmec.2020.103543.

[13] G. S. M. Hossein, F. Shirko, Free Vibration and Wave Propagation of Thick Plates Using The Generalized Nonlocal Strain Gradient Theory, J Theor Appl Vib Acous, Vol. 3, 2017, pp. 165-198.

[14] F. Ebrahimi, M. R. Barati, Hygrothermal Effects on Static Stability of Embedded Single-layer Graphene Sheets Based on Nonlocal Strain Gradient Elasticity Theory. J Thermal Stress, Vol. 42, 2019, pp. 1535-1550.

[15] M. R. Barati. Vibration Analysis of Porous FG Nanoshells with Even and Uneven Porosity Distributions Using Nonlocal Strain Gradient Elasticity. Acta Mech. Vol.229, 2018, pp. 1183–1196.

[16] L. H. Ma, L. L. Ke, J. N. Reddy et al., Wave Propagation Characteristics in Magneto-Electro-Elastic Nanoshells Using Nonlocal Strain Gradient Theory. Compos Struct, Vol. 199, 2018, pp. 10-23.

[17] H. Babaei, M. R. Eslami, on Nonlinear Vibration and Snap-through Buckling of Long FG Porous Cylindrical Panels Using Nonlocal Strain Gradient Theory, Compos Struct. Epub ahead of print 15 January 2021, Vol. 256, 2021, pp. 113125, https://doi.org/10.1016/j.compstruct.2020.113125.

[18] Q. Li, V. P. Iu, K. P. Kou, Three-dimensional Vibration Analysis of Functionally Graded Material Sandwich Plates, J Sound Vib, Vol. 311, 2008, pp. 498-515, https://doi.org/10.1016/j.jsv.2007.09.018.

[19] N. Lam, P. Mendis, T. Ngo, Response Spectrum Solutions for Blast Loading. Electron J Struct Eng. Vol.4, 2004, pp. 28–44.

## Appendix 1

***+) FG porous Type 1***

$$E_1 = E_c\left(h-h_{core}\right)+\frac{E_{mc}\left(h-h_{core}\right)}{k+1}+\frac{E_m h_{core}\left(\pi-2e_0\right)}{\pi},$$

$$E_2 = 0,$$

$$E_3 = \frac{E_c\left(h^3-h_{core}^3\right)}{12}+\frac{E_{mc}\left(2h^3+2kh^2h_{core}+k\left(k+1\right)hh_{core}^2-\left(k\left(k+2\right)+1\right)h_{core}^3\right)}{4k\left(k+2\right)\left(k+3\right)+1}$$
$$+\frac{E_m h_{core}^3\left(\pi^3-6e_0\pi^2+48e_0\right)}{12\pi^3},$$

***+) FG porous Type 2***

$$E_1 = E_c\left(h-h_{core}\right)+\frac{E_{mc}\left(h-h_{core}\right)}{k+1}+\frac{E_m h_{core}\left(\pi-2e_0\right)}{\pi},$$

$$E_2 = -\frac{E_m h_{core}^2 e_0\left(\pi-4\right)}{\pi^2},$$

$$E_3 = \frac{E_c\left(h^3-h_{core}^3\right)}{12}+\frac{E_{mc}\left(2h^3+2kh^2h_{core}+k\left(k+1\right)hh_{core}^2-\left(k\left(k+2\right)+1\right)h_{core}^3\right)}{4k\left(k+2\right)\left(k+3\right)+1}$$
$$+\frac{E_m h_{core}^3\left(\pi^3-6e_0\pi^2+192e_0-48\pi e_0\right)}{12\pi^3},$$

***+) FG porous Type 3***

$$E_1 = E_c\left(h-h_{core}\right)+\frac{E_{mc}\left(h-h_{core}\right)}{k+1}+E_m h_{core}\left(1-2\lambda_0 e_0\right),$$

$$E_2 = 0,$$

$$E_3 = \frac{E_c\left(h^3-h_{core}^3\right)}{12}+\frac{E_{mc}\left(2h^3+2kh^2h_{core}+k\left(k+1\right)hh_{core}^2-\left(k\left(k+2\right)+1\right)h_{core}^3\right)}{4k\left(k+2\right)\left(k+3\right)+1}$$

$$+\frac{E_m h_{core}^3\left(1-e_0\lambda_0\right)}{12},$$

**Appendix 2**

$$E_1 = \int_{-\frac{h}{2}}^{\frac{h}{2}} E(z)dz\,,\ E_2 = \int_{-\frac{h}{2}}^{\frac{h}{2}} zE(z)dz\,,\ \text{and}\ E_3 = \int_{-\frac{h}{2}}^{\frac{h}{2}} z^2E(z)dz$$

$$A_{11} = A_{22} = \frac{E_1}{1-\nu^2},\ A_{12} = A_{21} = \frac{\nu E_1}{1-\nu^2},\ A_{33} = \frac{E_1}{2\left(1+\nu\right)},$$

$$B_{11} = B_{22} = \frac{E_2}{1-\nu^2},\ B_{12} = B_{21} = \frac{\nu E_2}{1-\nu^2},\ B_{33} = \frac{E_2}{1+\nu}, B_{66} = \frac{E_2}{2\left(1+\nu\right)}$$

$$D_{11} = D_{22} = \frac{E_3}{1-\nu^2},\ D_{12} = D_{21} = \frac{\nu E_3}{1-\nu^2},\ D_{66} = \frac{E_3}{1+\nu},$$

$$T_1 = -\int_{-\frac{h}{2}}^{\frac{h}{2}} \frac{E\alpha\Delta T}{1-\nu}dz\,,\ T_2 = -\int_{-\frac{h}{2}}^{\frac{h}{2}} \frac{zE\alpha\Delta T}{1-\nu}dz$$

**Appendix 3**

$$h_{11} = -\frac{\pi^2\left(a^2l^2n^2\pi^2+b^2l^2m^2\pi^2+a^2b^2\right)}{4a^3b^3}\left(b^2m^2A_{11}+a^2n^2A_{33}\right)$$

$$h_{12} = -\frac{mn\pi^2\left(a^2l^2n^2\pi^2+b^2l^2m^2\pi^2+a^2b^2\right)}{4a^2b^2}\left(A_{12}+A_{33}\right)$$

$$h_{13} = \frac{m\pi^3\left(a^2l^2n^2\pi^2+b^2l^2m^2\pi^2+a^2b^2\right)}{a^4b^3}\left(b^2m^2B_{11}+a^2n^2B_{12}+a^2n^2B_{33}\right)$$

$$\eta_1 = \frac{I_0\left[a^2l^2mn^3\pi^4 + b^2l^2m^3n\pi^4 + a^2b^2mn\pi^2\right]}{4abmn\pi^2}$$

$$h_{21} = -\frac{mn\pi^2\left(a^2l^2n^2\pi^2 + b^2l^2m^2\pi^2 + a^2b^2\right)}{4a^2b^2}\left(A_{21} + A_{33}\right)$$

$$h_{22} = -\frac{\pi^2\left(a^2l^2n^2\pi^2 + b^2l^2m^2\pi^2 + a^2b^2\right)}{4a^3b^3}\left(a^2n^2A_{22} + b^2m^2A_{33}\right)$$

$$h_{23} = \frac{n\pi^2\left(a^2l^2n^2\pi^2 + b^2l^2m^2\pi^2 + a^2b^2\right)}{4a^3b^4}\left(b^2m^2B_{21} + a^2n^2B_{22} + b^2m^2B_{33}\right)$$

$$\eta_2 = \frac{I_0\left[a^2l^2mn^3\pi^4 + b^2l^2m^3n\pi^4 + a^2b^2mn\pi^2\right]}{4abmn\pi^2}$$

$$h_{31} = \frac{m\pi^3\left(a^2l^2n^2\pi^2 + b^2l^2m^2\pi^2 + a^2b^2\right)\left(B_{11}b^2m^2 + B_{21}a^2n^2 + 2B_{66}a^2n^2\right)}{a^4b^3}$$

$$h_{32} = \frac{n\pi^3\left(a^2l^2n^2\pi^2 + b^2l^2m^2\pi^2 + a^2b^2\right)\left(B_{12}b^2m^2 + B_{22}a^2n^2 + 2B_{66}b^2m^2\right)}{a^3b^4}$$

$$h_{33} = -\frac{1}{4}\frac{n^2\pi^4\left(\pi^2a^2l^2n^2 + \pi^2b^2l^2m^2 + a^2b^2\right)\left(D_{22}a^2n^2 + 2D_{66}b^2m^2\right)}{a^3b^5}$$

$$h_{34} = -\frac{1}{4}\frac{m^2\pi^2(\pi^2a^2l^2n^2 + \pi^2b^2l^2m^2 + a^2b^2)}{a^3b}$$

$$h_{35} = -\frac{1}{4}\frac{\left(a^2l^2n^2\pi^2 + b^2l^2m^2\pi^2 + a^2b^2\right)}{ab}$$

$$h_{36} = -\frac{1}{4}\frac{l^2\pi^2\left(\pi^2a^4n^4 + 2\pi^2a^2b^2m^2n^2 + \pi^2b^4m^4 + a^2b^4m^2\right)}{a^3b^3}$$

$$h_{37} = -\frac{ab\left[-1+(-1)^m\right]\left[-1+(-1)^n\right]}{nm\pi^2}$$